

PREDICTION OF ION DRIFT EFFECTS ON SPACECRAFT FLOATING POTENTIALS*

Jen-Shih Chang, S.M.L. Prokopenko, R. Godard and J.G. Laframboise
Centre for Research in Experimental Space Science and Physics Department
York University

ABSTRACT

The plasma environment of high-altitude spacecraft has been observed to involve ion drift velocities which sometimes become comparable to ion mean thermal speeds. Such drifts may cause an electrically isolated spacecraft surface to float at a substantially increased negative potential if it is simultaneously shaded and downstream relative to the drift direction. We present a calculation of upper and lower bounds on such potentials for a spherical spacecraft, based on the fact that ion collection on the spacecraft at its downstream point is bounded above by the corresponding current which would be collected if the spacecraft were an equipotential (i.e. were more attractive for ions elsewhere on its surface than it is in reality) and bounded below by the corresponding result for a sphere at space potential. The results show that (1) the ion speed ratio at which drift effects become "important" (i.e. change the floating potential by at least 10%) can be as low as 0.1, and may be decreased if the ambient electrons are non-Maxwellian; (2) the effects of ion speed ratio increase with increasing ion-to-electron temperature ratio; (3) negative floating potentials for drifting Maxwellian ion velocity distributions with speed ratio unity are typically about twice as large as the corresponding potentials for nondrifting conditions.

INTRODUCTION

If a spacecraft is exposed to ambient ions whose drift velocity U is comparable to or larger than their most probable thermal speed [ion speed ratio $S_1 = U/(2kT_1/m_1)^{1/2} \gtrsim 1$, where k is Boltzmann's constant and m_1 and T_1 are ion mass and assumed ion temperature], a large decrease in ion flux J_1 to downstream surfaces will occur. Unless such surfaces are able to expel surplus incident electron fluxes, e.g. by photoemission, their floating potentials will become substantially more negative as a result. If the ambient electron temperature T_e is simultaneously large or more generally the ambient electron energy distribution has a significant high-energy component, then large absolute increases in negative floating potentials will occur, with correspondingly increased arcing hazards. Even if T_e is relatively small, such effects may influence surface potentials enough to disturb particle and field measurements. S_1 values of order unity may be reached in the Earth's outer magnetosphere (Mauk 1975; DeForest 1977, Figs. 6 and 8); larger values are likely in the outer Jovian magnetosphere and magnetosheath (Goldstein and Divine 1977), and in the solar wind (Dessler 1967, Axford 1968, Manka 1973). In both outer

*work supported by the U.S. Air Force Office of Scientific Research under grant number AFOSR-76-2962.

magnetospheres, electron distributions having substantial high-energy components have been observed (DeForest and McIlwain 1971, Goldstein and Divine 1977).

A calculation of ion drift effects on the floating potential of the lunar surface has been done by Manka (1973), using a local-current-balance formulation. Parker (1978) has done exact numerical calculations of floating surface potentials for nonconductive finite cylindrical objects, including photoemission due to illumination of one end and ion drift parallel to the axis of symmetry.

In this paper, we have done an approximate calculation of ion drift effects on the floating potential of a shaded, downstream, electrically isolated surface element on a spherical spacecraft (Fig. 1), using a local-current-balance formulation which yields upper and lower bounds on such potentials. This formulation is an adaptation of that of Prokopenko and Laframboise (1977). The basis of the calculation is as follows: if one compares, on one hand, a situation wherein the entire spacecraft is at the same potential as the surface element in question, with, on the other hand, a more realistic situation wherein the rest of the spacecraft is at a less negative potential (Fig. 2), then in the latter case, the potential well surrounding the surface element will be steeper and less spatially extended, and the ion collection will in general be decreased. When $S_1 \neq 0$, this argument is subject to qualifications not present in the nondrifting case, for which it is rigorously true in a wide range of conditions (Laframboise and Parker 1973, Laframboise and Godard 1974). In particular, one can envision hypothetical asymmetric sheath potentials which would cause a high-speed-ratio ambient ion distribution to be focused onto the downstream point. We exclude such cases in what follows.

The most extreme example of steepening would be a potential profile which was equal to space potential almost to the spacecraft surface, then fell discontinuously to surface potential. In this limit, the surface element in question would collect just the downstream space-potential current corresponding to the given ion speed ratio. The downstream-point current-density values corresponding to a unipotential sphere at, respectively, the potential of the surface element and space potential may therefore be regarded as upper and lower bounds on the actual current collection at that potential, the upper bound being subject to the above-mentioned qualifications. The resulting values of local floating surface potential may correspondingly be regarded as upper and lower bounds on more realistic values of this quantity. The above-mentioned upper and lower bounds on current correspond, respectively, to the "three-dimensional" and "one-dimensional" velocity-space cutoffs considered by Prokopenko and Laframboise (1977) for nondrifting situations.

THEORY OF LOCAL ION COLLECTION ON A UNIPOTENTIAL SPHERE

We assume a collisionless plasma with a drifting Maxwellian ion velocity distribution and negligible magnetic field, containing a fully charge-absorbing, unipotential, spherical electrode. We assume that Debye length $\lambda_D \gg$ electrode radius r_s . In the resulting spherically symmetric Laplace potential $\phi(r) = \phi_s r_s / r$, the nondimensional ion current density at the electrode surface is (Godard 1975, p. 31)

$$j_i = \int_{\max(0, \chi_s)}^{\infty} \int_0^{\beta - \chi_s} \exp(-\beta - 2S_1 \beta^{1/2} \cos \mu \cos \theta - S_1^2) I_0(2S_1 \beta^{1/2} \sin \mu \sin \theta) d\Omega d\beta \quad (2.1)$$

where $\chi_s = q\phi_s/kT$, $\beta = E/kT$, $\Omega = L^2/(2mr^2 kT)$, $j = J/[N_\infty q(kT/2\pi m)^{1/2}]$, I_0 is the modified Bessel function of zero order, N_∞ is number density far from the electrode, μ is angular surface position coordinate measured from the upstream direction, θ is change in direction of the radius vector of a particle as it moves from infinity to radial distance r_s , and θ is related to particle energy E , angular momentum L , charge q and the potential profile $\phi(r)$ by the following expression (Goldstein 1950, Ch.3):

$$\theta = \int_{r_s}^{\infty} Ldr / \{r^2 [2mE - 2mq\phi(r) - L^2/r^2]\}^{1/2} \quad (2.2)$$

We have computed j_i by integrating Eq. (2.1) numerically. For the given Laplace potential, Eq. (2.2) can be integrated analytically. We obtain

$$\theta = \sin^{-1}[(2\Omega + \chi_s)/(\chi_s^2 + 4\beta\Omega)^{1/2}] - \sin^{-1}[\chi_s/(\chi_s^2 + 4\beta\Omega)^{1/2}] \quad (2.3)$$

For space potential ($\chi_s = 0$), Eq. (2.1) can be integrated analytically. The result is (Tsien 1946)

$$j_i = \pi^{1/2} S_1 \cos \mu [1 + \operatorname{erf}(S_1 \cos \mu)] + \exp(-S_1^2 \cos^2 \mu) \quad (2.4)$$

Figure 3 shows results obtained for the ion current density $j_{i\pi}$ at the downstream point $\mu = \pi$, as a function of S_1 , with χ_s as a parameter, where $\chi_s = e\phi_s/kT_i \leq 0$ and $e \equiv q_i$. As expected, $j_{i\pi}$ decreases with increasing S_1 and increases with increasing $|\chi_s|$. In Fig. 4, the same results are graphed logarithmically as functions of χ_s . Figure 4 shows that these results may be approximated with an error $\lesssim 5\%$ by power-law relations of the form

$$j_{i\pi}(\chi_s) = j_{i\pi}(\chi_s = 0) + A_\pi |\chi_s|^{\alpha_\pi} \quad \chi_s \leq 0 \quad (2.5)$$

The resulting S_1 dependence of the coefficients A_π , α_π and $B_\pi \equiv j_{i\pi}(\chi_s = 0)$ is shown in Fig.5.

RESULTS AND DISCUSSION

Upper and lower bounds on negative downstream-point floating potentials for a shaded, isolated surface element, obtained by numerical solution of the equation $J_i + J_e = 0$, are shown in Fig. 6 for various ion-to-electron temperature ratios $\epsilon = T_i/T_e$. Here we have assumed that ambient electrons are Maxwellian, and that J_i is given alternatively by Eq. (2.5) with Fig. 5, and by Eq. (2.4), yielding upper and lower bounds on ion current, corresponding respectively to "three-dimensional" and "one-dimensional" ion velocity-space cutoffs (Sec. 1). We have also assumed that secondary, backscattered, and photoemitted electron currents are zero. The lower-bound results are subject to the qualifications noted in Sec. 1. The dashed lines in Fig. 6 represent floating potentials for the nondrifting case $S_1 = 0$. At ion speed ratios larger than those shown, the situation becomes complicated by electron speed ratio effects, especially at larger values of ϵ . In Fig. 6 we see that at larger values of ϵ , effects of S_1

become important at smaller S_1 values.

In Fig. 7, upper and lower bounds are shown which are similar to those of Fig. 6, except that instead of Maxwellian electron velocity distributions, we have used the "quiet" and "disturbed" electron distributions measured by Shield and Frank (1970) and DeForest and McIlwain (1971) respectively in the Earth's outer magnetosphere, and approximated by Knott (1972), as described by Prokopenko and Laframboise (1977) and Laframboise and Prokopenko (1978). The ion temperatures used are 11.6 eV and 2.43 keV, respectively. These values were obtained by integrating the electron velocity distributions to find $N_{e\infty}$, equating $N_{i\infty}$ to the result, then assuming that the ions were Maxwellian and that the ratio of ion to electron random fluxes was 0.025. This procedure differs from that used by Knott (1972) and Prokopenko and Laframboise (1977), in which an ion-to-electron random flux ratio of 0.025 and an ion temperature of 1 keV were assumed simultaneously, thereby violating ambient charge neutrality in general. The corresponding electron mean energies are 270 eV and 8.78 keV. The method used for calculating electron currents is described in Prokopenko and Laframboise (1977). We see that S_1 effects become important at smaller S_1 values in "quiet" magnetospheric conditions. The ratio of ion to electron mean energies implied by the above data is also larger in "quiet" conditions, corresponding to the dependence of S_1 effects on ϵ noted in Fig. 6. The "quiet" and "disturbed" distributions also differ substantially in shape (Knott, 1972, Figs. 1 and 2b). The onset of "significant" drift effects (i.e. floating potential changes $\gtrsim 10\%$) is seen to occur at S_1 values as low as 0.1, depending on conditions. It occurs at lower S_1 values in the presence of the "quiet" distribution than in any of the other cases shown in Figs. 6 and 7. In Figs. 6 and 7, negative floating potentials for $S_1=1$ are in most cases about twice as large as the corresponding potentials for nondrifting situations.

REFERENCES

- Axford, W.I. (1968), Observations of the interplanetary plasma, Space Sci. Rev. 8, 331-365.
- DeForest, S.E. (1977), The plasma environment at geosynchronous orbit. In: Proc. USAF-NASA Spacecraft Charging Technology Conference, C.P. Pike and R.R. Lovell, Editors, Report No. AFGL-TR-77-0051, Air Force Geophysics Laboratory, Hanscom AFB, Massachusetts/NASA TMX-73537, Lewis Research Center, Cleveland, Ohio, pp. 37-52.
- DeForest, S.E., and McIlwain, C.E. (1971), Plasma clouds in the magnetosphere, J. Geophys. Res. 76, 3587-3611.
- Dessler, A.J. (1967), Solar wind and interplanetary magnetic field, Rev. Geophys. 5, 1-41.
- Godard, R. (1975), A symmetrical model for cylindrical and spherical collectors in a flowing collisionless plasma, Ph.D. Thesis, York University, Toronto.
- Goldstein, H. (1950), Classical Mechanics, Addison-Wesley Pub. Co., Reading, Massachusetts.
- Goldstein, R. and Divine, N. (1977), Plasma distribution and spacecraft charging modeling near Jupiter. In: Proc. USAF-NASA Spacecraft Charging

Technology Conference, C.P. Pike and R.R. Lovell, Editors, Report No. AFGL-TR-77-0051, Air Force Geophysics Laboratory, Hanscom AFB, Massachusetts /NASA TMX-73537, Lewis Research Center, Cleveland, Ohio, pp. 131-141.

- Knott, K. (1972), The equilibrium potential of a magnetospheric satellite in an eclipse situation, Planet. Space Sci. 20, 1137-1146.
- Laframboise, J.G., and Godard, R. (1974), Perturbation of an electrostatic probe by a spacecraft at small speed ratios, Planet. Space Sci. 22, 1145-1155.
- Laframboise, J.G., and Parker, L.W. (1973), Probe design for orbit-limited current collection, Phys. Fluids 16, 629-636.
- Laframboise, J.G., and Prokopenko, S.M.L. (1978), Predictions of high-voltage differential charging on geostationary spacecraft, Paper 4.4, 1978 Ionospheric Effects Symposium, Arlington, January 1978 (proceedings in press).
- Manka, R.H. (1973), Plasma and potential at the lunar surface. In: Photon and Particle Interactions with Surfaces in Space, R.J.L. Grad, Editor, D. Reidel Pub. Co., Dordrecht, Holland, pp. 347-361.
- Mauk, B. (1975), Magnetospheric substorm pitch angle distribution, EOS 56, 423.
- Parker, L.W. (1978), Potential barriers and asymmetric sheaths due to differential charging of nonconducting spacecraft. Report No. AFGL-TR-78-0045, Air Force Geophysics Laboratory, Hanscom AFB, Massachusetts.
- Prokopenko, S.M.L., and Laframboise, J.G. (1977), Prediction of large negative shaded-side spacecraft potentials. In: Proc. USAF-NASA Spacecraft Charging Technology Conference, C.P. Pike and R.R. Lovell, Editors, Report No. AFGL-TR-77-0051, Air Force Geophysics Laboratory, Hanscom AFB, Massachusetts/NASA TMX-73537, Lewis Research Center, Cleveland, Ohio, pp. 369-387.
- Shield, M.A., and Frank, L.A. (1970), Electron observations between the inner edge of the plasma sheet and the magnetosphere, J. Geophys. Res. 75, 5401-5414.
- Tsien, H.S. (1946), Superaerodynamics, mechanics of rarefied gases, J. Aero. Sci. 13, 653-664.

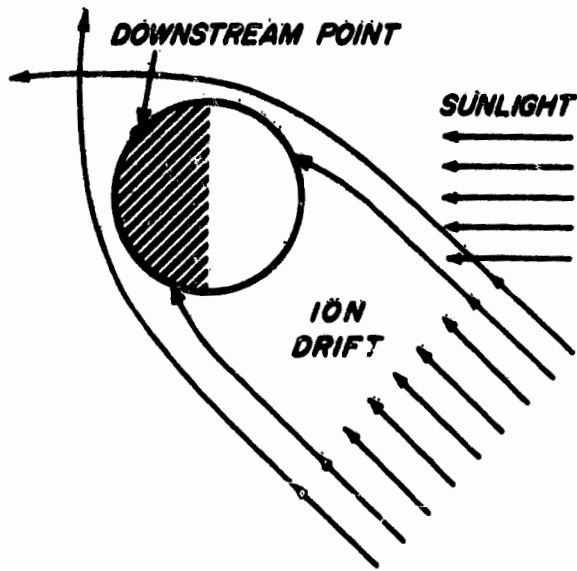


Figure 1. Spherical spacecraft with downstream point (relative to ion drift direction) shaded.

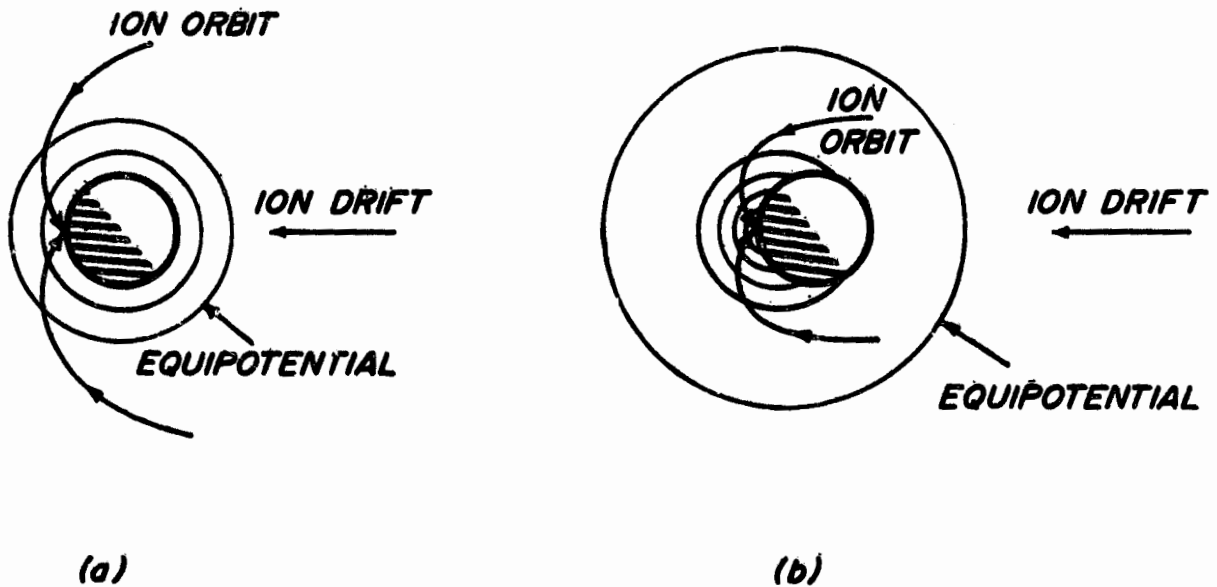


Figure 2. (a) Hypothetical symmetric equipotentials around a spherical spacecraft (b) nonsymmetric equipotentials around the same spacecraft.

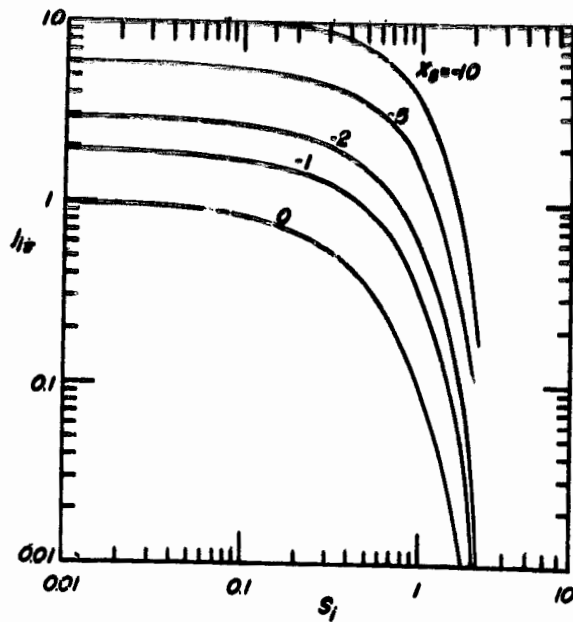


Figure 3. Nondimensional downstream-point ion current density $j_{i\pi} = J_{i\pi} / [N_{\infty} e (kT_1 / 2\pi m_1)^{1/2}]$ as a function of ion speed ratio $S_1 = U / (2kT_1 / m_1)^{1/2}$ for various nondimensional surface potentials $\chi_s = e\phi_s / kT_1$, assuming spherical geometry, zero magnetic field, uniform surface potential, collisionless large-Debye-length conditions, and drifting Maxwellian ions. For $S_1 \rightarrow 0$, $j_{i\pi} \rightarrow 1 + |\chi_s|$ when $\chi_s < 0$.

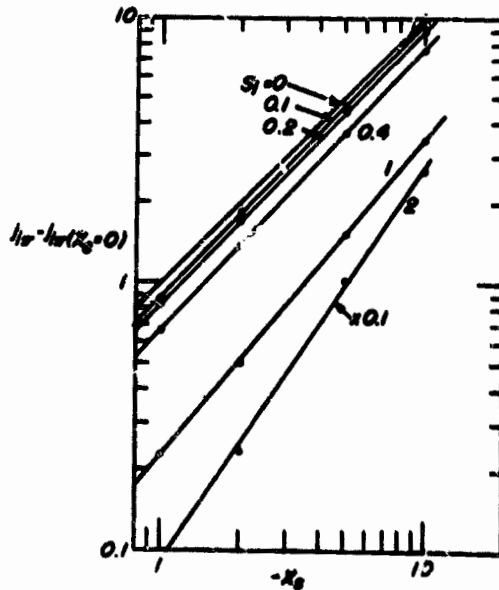


Figure 4. Nondimensional downstream-point ion current density $j_{i\pi}$ as a function of surface potential χ_s for various ion speed ratios S_1 , for the same conditions as in Fig. 3. The straight lines shown are power-law approximations.

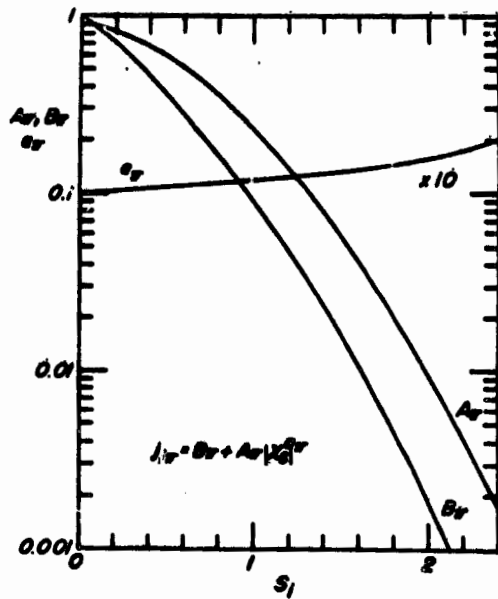


Figure 5. Dependence of the power-law coefficients A_{π} , B_{π} and α_{π} on ion speed ratio S_1 .

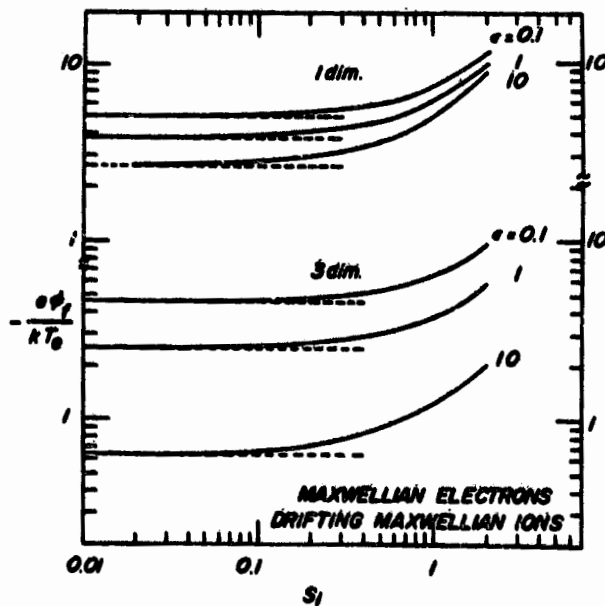


Figure 6. Upper and lower bounds on floating potential ϕ_F at shaded downstream point of spacecraft, as a function of ion speed ratio S_1 for various ion-to-electron temperature ratios ϵ , for Maxwellian electrons and drifting Maxwellian ions, for 1-dimensional and 3-dimensional ion velocity space cutoffs.

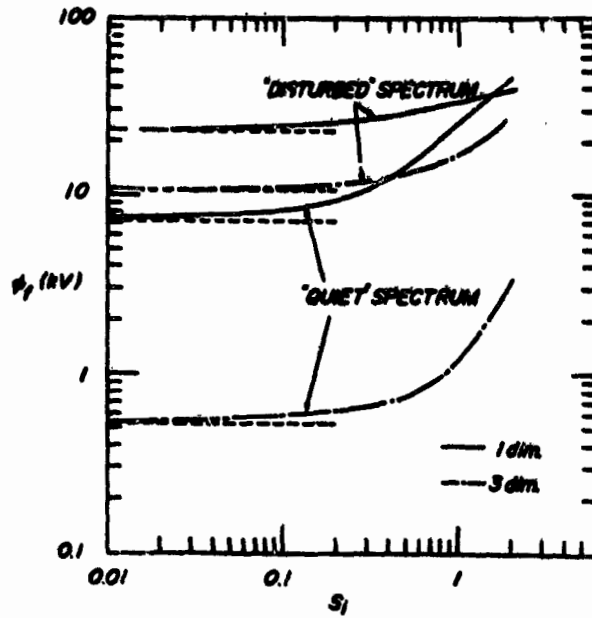


Figure 7. Upper and lower bounds on floating potential ϕ_f at shaded downstream point of spacecraft, as a function of ion speed ratio S_i for "disturbed" and "quiet" electron velocity spectra representing geostationary orbit conditions, for 1-dimensional and 3-dimensional ion velocity space cutoffs.